## Title
Surface finishing of die and tool steels via plasma-based electron beam irradiation



## Journal
Journal of Materials Processing Technology, 180(1-3)

## ISSN
0924-0136

## Authors
Yu, Z
WANG, ZHIGANG
Yamazaki, Kazuo
et al.

## Publication Date
2006-12-01

Peer reviewed

# Surface finishing of die and tool steels via plasma-based electron beam irradiation

Zhanbo Yu[a], Z.G. Wang[b*], K. Yamazaki[b], S. Sano[a]

[a]Sodick Co. Ltd, Yokohama, Japan

[b]Department of Mechanical & Aeronautical Engineering, University of California, Davis, One Shields Avenue, Davis, CA, 95616, USA

**Abstract:** The plasma-based electron beam (PBEB) irradiation with a maximum diameter of 60 mm has been used to smoothen the workpiece surface. After PBEB irradiation, the machined surface roughness is reduced, and its corrosion resistance is improved. However, for die and tool steels, some craters still exist on the surface after PBEB irradiation, which remain a big problem for the roughness improvement and quality control of the machined surfaces. In this study, four types of work materials have been tested during PBEB irradiation. The effects of non-metallic inclusions (MnS and carbide) and impurities on the generation of craters were investigated. In addition, craters formed on the work materials with different nitrogen concentrations have also been observed after PBEB irradiation. Finally, a case study is given, and it is found that PBEM irradiation can achieve good surface finish of die steel materials.

**Keyword:** Electron beam, surface roughness, die steel, tool steel, crater

## 1. Introduction

Recently, energy beam processing has been widely used in industries to machine difficult to cut

* Corresponding author. Tel: +1-530-752 6086; fax: +1-530-752 4158.
Email address: zgwang@ucdavis.edu

materials and produce miniaturized components. The material removal is achieved by increasing the internal energy of atoms in the workpiece, consequently the work material with high internal energy is removed atom by atom, or atom cluster by atom cluster. Thus, this method is also called 'atomic-scale' processing [1]. Another significant advantage of energy beam processing is that there is no limitation imposed by workpiece hardness and ductility. So this technique has a potential to be a new way to machine hard die steels and aeronautical alloys. Among all energy beam processing techniques, the electron beam (EB) process gains more and more attention nowadays, because the electron beams can be controlled easily and accurately, and EB beam power is generated at very considerately high efficiency. Moreover, in most cases, this EB process happens in a vacuum or near vacuum condition, thus the oxidation of the hot workpiece with the oxygen is eliminated. Therefore, the EB process has been successfully used for welding, brazing, alloying, and other types of surface treatment [1-7].

Traditionally, EB processing employs electrons from an electron gun, then the electrons are focused into beams with a very small diameter and projected onto a solid [1, 2]. The key feature of this method is to use the electrons with high kinetic energies. The high-speed electrons transfer their kinetic energies to the surface layer of the workpiece when they penetrate into the solid target. Under this effect of energy transfer, the workpiece surface is heated, and then melted with the further increase of the temperature. Finally, the workpiece material is removed via evaporation. Because the effective diameter of the traditional EB is in micron and sub-micron scale, a large amount of beam scanning is needed in case of large area treatment. Therefore, it needs longer machining time with this method. Recently, high-speed EB scanning has been used in the surface treatment to reduce the machining time [3, 4]. However, due to the small spot size of EBs, overlapping of the scanning tracks is indispensable. This overlapping region of scanning tracks shows increased crack probability [5], and it also affects the machined surface roughness.

In order to avoid the above limitations, the large area plasma-based EB (PBEB) has been used to machine die and tool steels in this paper. This PBEB has an effective diameter of 60 mm, which is significantly larger than that of the traditional focused EB. Using this proposed method, it is possible to smooth the surface of an area with a maximum diameter of 60 mm without beam scanning. The irradiation shot duration is 2-4 μs, so the die and tool steels can be machined within a very short time.

## 2. Recent study of the plasma-based EB process

Okada et al [6] used EB irradiation to smoothen the electric discharge machined (EDM-ed) surface of SKD11 die steels. The surface profiles before and after EB irradiation are shown in Fig. 1 (a) and (b), respectively. After EB irradiation, it was observed that the surface roughness Ry was reduced from initial value of 6 μm to 1 μm in an area with a diameter of 60 mm within several seconds [6].

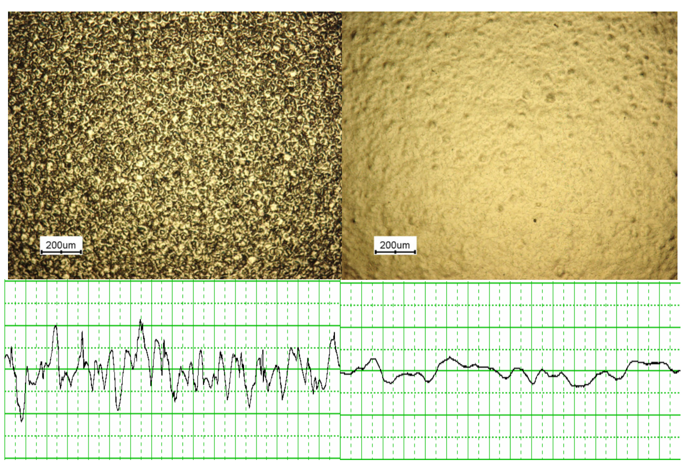


(a) EDM (Ry =5μm)    (b) EB irradiation (Ry =1.13μm)

**Fig. 1 Profiles of SKD11 workpiece surfaces before and after EB irradiation [6]**

However, sometimes micro-craters are found on the machined surface after the EB irradiation as shown in Fig. 2 [6]. The existence of these craters after EB irradiation affects surface roughness and quality control of the workpiece. Currently, the factors that affect the generations of these micro-craters on die and tool steels are still unknown. Therefore, in this paper, PBEB irradiation process was conducted on several metal alloys in order to investigate the factors that generate craters and find suitable materials for this process.

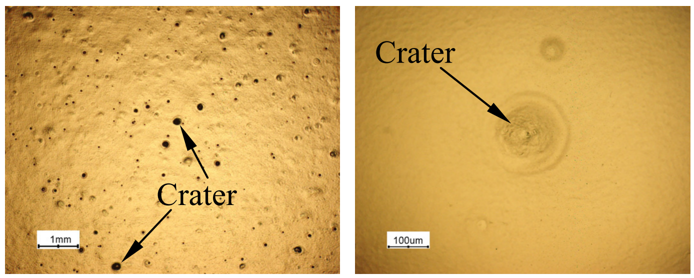


(a) (b)

**Fig. 2 Micrograph of SKD11 workpiece surfaces after EB irradiation [6]**

## 3. Experimental methodology

### 3.1 Experimental setup

The generation of high energy density PBEB is shown in Fig. 3 [7]. The workpiece is mounted on a worktable inside the vacuum chamber. This vacuum chamber is firstly evacuated to 0.03Pa; thereafter argon gas is added until the air pressure inside it reaches 0.05 Pa. Then, a pulse current is supplied into the solenoid coil to generate magnetic field between the cathode and anode. In this method, there is no injection of electrons or photons from the outside of the chamber to generate the initial plasma. And the solenoid magnetic field is important for the plasma preparation, because the plasma can be kept at a low density with this magnetic field. When the magnetic field produced by the solenoid coil reaches to its highest strength, a pulse voltage is applied to the anode. Then, electrons are generated by the Penning effect and start to move towards the anode. Under the effect of magnetic field generated by the solenoid, electrons move spirally and collide with argon gas atoms. Due to repetitious collisions between the electrons and argon gas atoms, argon atoms are ionized, and then the plasma is generated. The plasma diffuses in the space between the cathode and anode. When the plasma intensity reaches its maximum value, a high negative voltage pulse is loaded to the cathode. Under the effect of the high voltage on the cathode, a plasma layer is produced near the cathode. Then the electrons are accelerated by the high-electric field due to electric double layer formed near the cathode. Finally, the accelerated electrons pass through the anode plasma and penetrate into the workpiece surface with an effective diameter of 60 mm. The generated electron beam has a pulse duration of 2-4 μs, peak current of 40 kA, and the maximum energy density of 15 J/$cm^2$. The beam conditions used in the experiments are listed in Table 1.

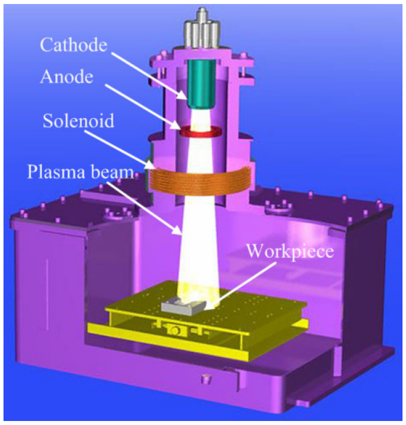


**Fig. 3 A schematic illustration of high current high enthalpy PBEB machine [7]**

**Table 1 Electron beam conditions used in this study**

| | |
|---|---|
| Acceleration voltage (kV) | 28 |
| Number of pulse | 20 |
| Discharge duration (μs) | 2-4 |
| Discharge frequency (Hz) | 0.2 |
| EB diameter (mm) | 60 |

### 3.2 Workpiece materials

To investigate the effects of non-metallic inclusion (MnS), large carbide, nitrogen gas element, refinement method (vacuum melting) on the crater formation and surface roughness, the following materials have been tested.

Table 2 shows the chemical composition of NAK55 and NAK80 [8]. Both materials are the prehardened steel for plastic molds. In order to increase the machinablity and wear resistance, most of die/mold materials contain certain amount of sulfur or carbide. Sometimes, these non metallic inclusions may be included during the purification process. NAK55 contains sulfur additive for increasing machinability. While in order to increase its machinability for electric discharge machining (EDM) processes, NAK80 does not contain any sulfur.

**Table 2 Chemical composition of NAK55 and NAK80 (wt %)**

<table>
<tr><th>Materials</th><th>C</th><th>Si</th><th>Ni</th><th>Cu</th><th>Mo</th><th>Al</th><th>Mn</th><th>S</th></tr>
<tr><td>NAK55</td><td>0.15</td><td rowspan="2">0.30</td><td rowspan="2">3.00</td><td rowspan="2">1.00</td><td rowspan="2">0.30</td><td rowspan="2">1.00</td><td rowspan="2">1.50</td><td>0.10</td></tr>
<tr><td>NAk80</td><td>0.20</td><td>—</td></tr>
</table>

In order to investigate the effects of the carbide on the generation of craters, two samples of high alloy tool steels SKD11 and DC53 have been tried, and their chemical composition is given in Table 3 [8]. The large carbide in these steels is helpful to improve wear resistance. Generally, the contents of large carbide increase with the increase of the amount of C, Cr and Mo.

**Table 3 Chemical composition of SKD11 and DC53 (wt %)**

| Material | C | Si | Mn | S | Cr | Mo | V |
|---|---|---|---|---|---|---|---|
| SKD11 | 1.40 | 0.3 | 0.4 | 0.002 | 11.5 | 1.0 | 0.3 |
| DC53 | 1.00 | 1.0 | 0.4 | 0.002 | 8.0 | 2.0 | 0.3 |

In addition, four SKD61 die steel samples without large carbides were also tested in the study;

their chemical composition is listed in Table 4 [8]. To investigate the influence of gas element, before experiments, these four SKD61 samples as the base material were firstly melted, and then the melted metal were exposed to nitrogen gas with the gas content adjustment. Under this condition, nitrogen is solved in the solid solution in the form of elementary atom not of a nitride compound. The absorbed nitrogen atom cannot be transformed to gas if the sample is heated at a temperature less than its melting point. The samples with a dimension of 10×20×5 mm were obtained by grinding, after quenching to obtain a hardness of HRC50

**Table 4 Chemical composition of four SKD61 samples (wt %)**

<table>
<tr><th>Material</th><th>C</th><th>Si</th><th>Mn</th><th>Cr</th><th>Mo</th><th>N</th></tr>
<tr><td>Sample 1</td><td rowspan="4">0.35</td><td rowspan="4">0.05</td><td rowspan="4">0.60</td><td rowspan="4">5.50</td><td rowspan="4">3.0</td><td>0.016</td></tr>
<tr><td>Sample 2</td><td>0.046</td></tr>
<tr><td>Sample 3</td><td>0.103</td></tr>
<tr><td>Sample 4</td><td>0.138</td></tr>
</table>

Finally, the mold steels HPM38 and HPM38S purified with vacuum melting were used in this study, and the chemical composition of HPM38 and HPM38S, and the nonmetal inclusions in these two materials are shown in Tables 5 and 6 [9], respectively. As for the determination of number and size of nonmetal inclusion particles in these two materials, two standard test methods, JIS-G0555 and ASTM-E45, are used. Normally, HPM38 is used for plastic dies because of its high hardness, high corrosion resistance and its mirror finishability. HPM38S is produced with a twice vacuum melting so as to reduce the nonmetallic inclusions. Table 6 shows that less nonmetallic impurities exist in HPM38S. Thus, HPM38S can be used to produce super-mirror surfaces with a surface roughness of less than 0.01 μm [9]. During experiments, after preliminary treatment by quenching to obtain a hardness of HRC40, test samples with a dimension of 50×50×20 mm were obtained by grinding.

**Table 5 Chemical composition of HPM38 and HPM38S (wt %)**

| Material | C | Si | Mn | Cr | Mo | S |
|---|---|---|---|---|---|---|
| HPM38 | 0.38 | 0.45 | 0.4 | 13.5 | 0.5 | 0.01 |
| HPM38S | | | | | | |

**Table 6 Testing results of nonmetal inclusion particles in HPM38 and HPM38S**

| Material | JIS G0555 | | ASTM E45-97 | | | |
|---|---|---|---|---|---|---|
| | dA | d(B+C) | A | B | C | D |
| | | | T/H | T/H | T/H | T/H |
| HPM38 | 0 | 0.004 | 0.0/0.0 | 0.0/0.0 | 0.0/0.0 | 0.5/0.5 |
| HPM38S | 0 | 0 | 0 | 0 | 0 | 0 |

## 4. Results and discussion

PBEB irradiation used in this study is a heating process. During the irradiation, firstly the workpiece surface is melted to a depth of about several micro-meters. Then, the melted liquid is vaporized with the further increase of the temperature. After evaporation, the temperature starts to decrease. When the temperature is reduced below the melting point of the target metal, the melted metal is solidified. Thus, one iteration of PBEB irradiation is finished. Due to extremely high instantaneous energy density and short irradiation time in PBEB process, only a very thin layer of machined surface is removed without any change in the substrate materials. Therefore, the machined surface is smoothened with this iterative procedure. There are so many factors involved in this process, such as beam conditions and material properties. In this study, the main purpose is to investigate the effects of material properties on the EB process.

### 4.1 Effects of non metallic inclusion MnS

Firstly, three types of pretreatment processes: grinding, EDM, in-water wire electro-discharge machining (WEDM), were applied on NAK55 and NAK80 to get a dimension of 50×50×20 mm. Then, PBEB process is used to machine the surfaces obtained from the preliminary treatment. After 20 irradiation shots, the microscopic figures of machined surfaces are shown in Fig. 4. After the EB irradiation for all three pretreatment conditions, less number of craters and the smoother machined surface were observed on NAK80 test sample, which does not contain the inclusion of MnS. Both samples have a similar composition except the existence of S in NAK55. Generally, if there is no MnS inclusion in the material, the inclusion of S helps to form MnS, and the amount of MnS is related to the amount of S. MnS has a lower melting point than that of the metal matrix of steels [10]. Thus, due to the lower melting point of the non metallic inclusions MnS, the melting and evaporation occur locally and the solidification happens before the metal surface is completely flat. Under this condition, it may generate craters on the machined surface. From the observation of larger number of craters on NAK55, it can be assumed that the existence MnS causes the generation of craters.

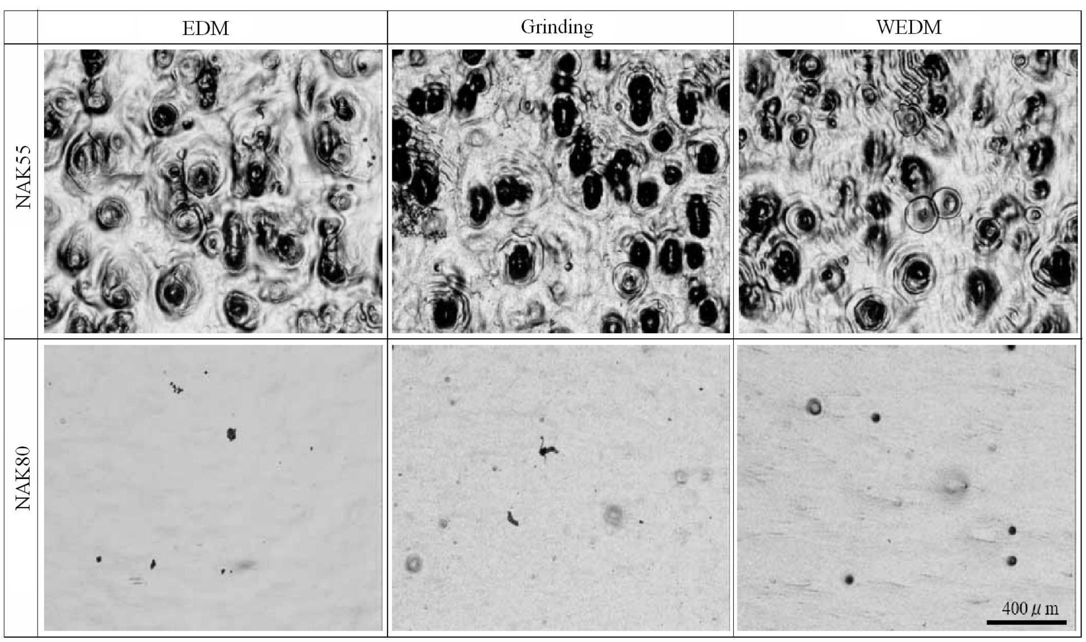


**Fig. 4 Microscope figures of machined surfaces of NAK55 and NAK80**

### 4.2 Effects of large carbides

To investigate the effects of large carbide on the crater generation, two tool steel samples, SKD11 and DC53, have been tried. Before experiments, the EDM-ed sample with a dimension of 50×50×20 mm is firstly heat-treated by quenching to obtain hardness of HRC62. Figure 5 shows optical microscopic figures of machined surfaces after 20 EB irradiation shots. From Fig. 5, it can be seen that more craters are observed on the SKD11 sample. Then, the irradiated surfaces were etched by the nital acid to observe their microstructure. The cross section of these two test samples after etching their surface layer is shown in Fig. 6. It was found that SKD11 has higher contents of large carbides than DC53. In the case of SKD11, the cross section of the surface layer is not continuous due to existence of craters. However, fewer craters were found on DC53, and its surface layer becomes more homogenous. Therefore, the existence of large carbide may cause the formation of craters. The lower amount of large carbide, the smoother surface can be obtained.

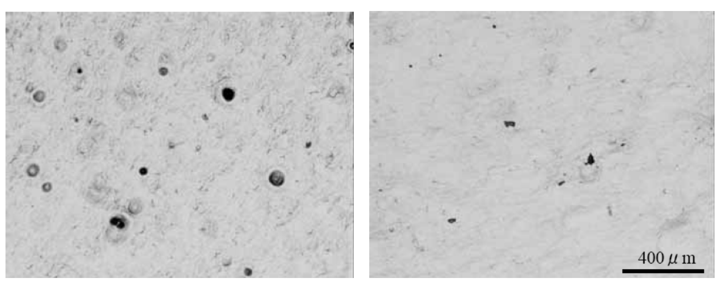


(a) SKD11 (b) DC53

**Fig. 5 Morphology of SKD11 and DC53 workpiece surfaces after PBEB irradiations**

### 4.3 Effects of nitrogen gas element

Four SKD61 die steel samples with high thermal fatigue strength were also tested in this study. The content of sulphur in these four materials is less than 0.002%; therefore the effect of MnS can be neglected. In addition, due to the lower content of C, the possibility of forming the carbide is very low. Therefore, it can be considered that the crater generation is not noticeably resulted from large carbides. During experiments, 20 irradiation shots were applied on Samples 1, 2, 3 and 4 within the same time, the machined surface profiles are shown in Fig. 7. Initially, the number of craters on the irradiated surface reduces gradually with the increase of the content of nitrogen. However, with the further increase of the nitrogen content, more craters and a crack were found on the machined surface, as shown in Sample 4. Based on the experimental results, it can be seen that, for PBEB process, a certain amount of nitrogen gas content is helpful to reduce the number of craters on the machined surface. Canadinc et al [11] found that nitrogen interstitials stabilize the Fe-Mn FCC structure, and interstitial nitrogen is a more effective strengthener than interstitial carbon. However, when the nitrogen content reaches a certain level, nitrogen concentrations significantly increase the hardening rate and reduce deformation hardening [11]. This may be the reason for the generation of cracks in Fig. 7 (d).

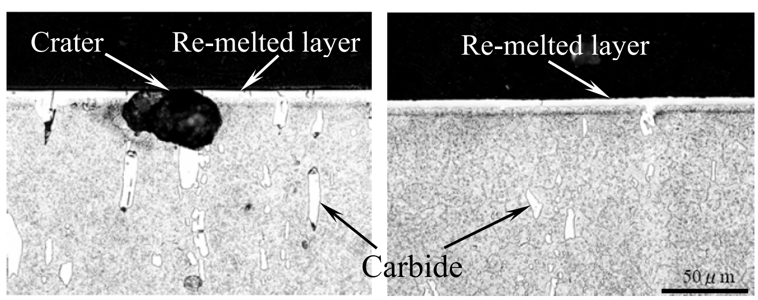


(a) SKD11 (b) DC53

**Fig. 6 Morphology of Cross sectional surface of SKD11 and DC53**

**4.4 Effects of the refinement method**

Figure 8 shows the optical microscopic pictures of the machined surfaces after 20 PBEB irradiation shots. It can be seen that HPM38S, which was made with the dual vacuum melting, has less number of craters. During the vacuum melting, content of nitrogen and oxides such as alumina in the material is reduced. However, in a single vacuum melting, somehow there still exists some nonmetallic impurity inside the work material. Through double vacuum melting, the impurity in the material can be further reduced. Thus, it can be concluded that the double vacuum melting or casting can help to avoid crater formation.

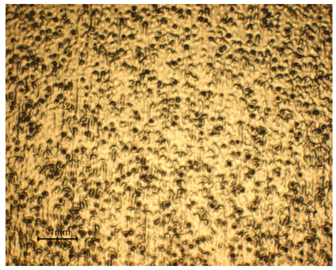
(a) Sample 1

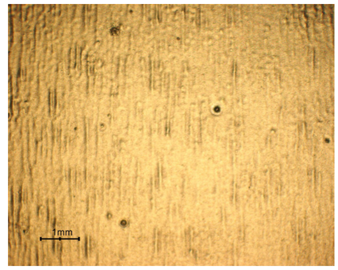
(b) Sample 2

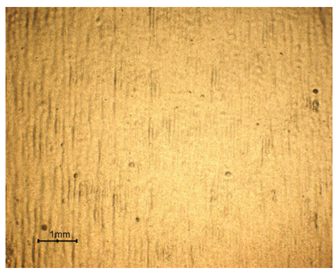
(c) Sample 3

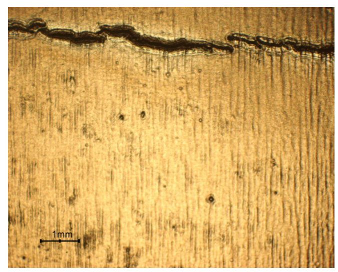
(d) Sample 4

**Fig. 7 Morphology of four SKD61 test samples' surfaces after PBEB irradiations**

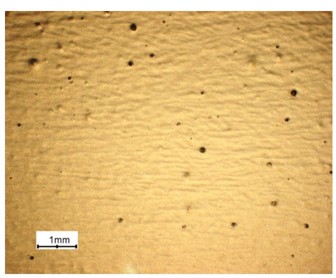

(a) HPM38

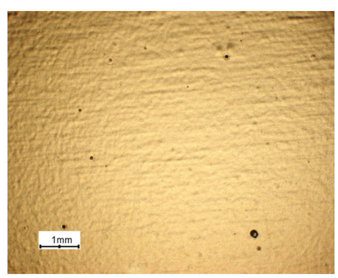

(b) HPM38S

**Fig. 8 Morphology of HPM38 and HPM38S workpiece surfaces after EB irradiations**

### 4.5 Corrosion resistance of machined surface

The corrosion resistance of machined surface of SKD11 was evaluated with the salt spray. During the experiment, two test samples were kept in the sink at 35$^{o}$C, where the two circular areas on the samples as shown in Fig. 9 were machined with EDM and EDM + PBEB irradiation, respectively. In the salt spray test, 5% salt fog was sprayed to these two circular areas continuously for 30 minutes. The EDM-ed circular area became rusty, while no rust was observed on the PBEB irradiated surface. So the corrosion resistance has been greatly improved by EB irradiation, similar results have also been found in [12]. This may be attributed to the uniform material structure of the remelted surface layer after PBEB irradiation. Figure 6 shows that there still exists a bright layer at the work material surface even after etching with the nital acid. This layer was formed after melting and consolidation of the work material at the top surface during PBEB irradiation process, and it is difficult to be etched. Therefore, the existence of this layer reiterates that the corrosion resistance of the PBEB machined surface has been greatly improved.

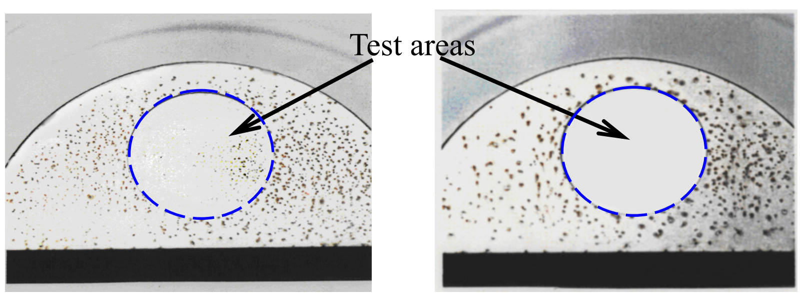


(a) EDM-ed circular area; (b) PBEB irradiated circular area

**Fig. 9 Surface profiles of EDM-ed and PBEB irradiated surface after the salty spray corrosion test**

**5. Case study**

Figure 10 shows an example of surface treatment on a crimper for wire terminal pressing, and the test material is SKD11. In Section 4.2, it was found that the high content of carbide results in craters on the machined surface. In order to reduce the detrimental effect of the carbide content, PBEB with a low energy density of 4.64 J/cm$^2$ was used in this test, and totally 20 irradiation shots were applied on the test sample. If this sample is manufactured using wire-EDM together with the hand polishing, and it takes around 3 hours. However, with PBEB irradiation proposed in this study, the process can be finished within 15 minutes. At the same time, the surface roughness (Ry) can be reduced from 1.16μm to 0.76μm, and the glossiness of surface has also been improved. Therefore, PBEB irradiation would be an efficient alternative for the finishing process of die and tool steels.

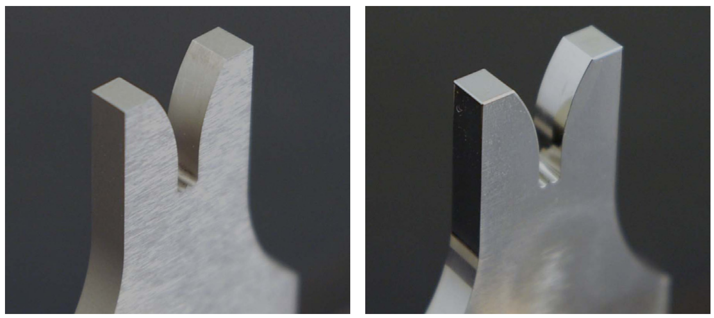

(a) Wire-EDM (b) PBEB irradiated

**Fig. 10 SKD11 test sample before and after PBEB irradiation process**

**6. Conclusions**

In this research, firstly the crater formation in the EB irradiation process of different materials is investigated. Then the corrosion resistance was carried out followed by a case study. Based on the obtained results, the following conclusions can be drawn:

1. More craters appear on machined surfaces for NAK55 with MnS inclusions.
2. The lower content of the large carbide, the fewer craters formed.
3. Nitrogen gas element in the metal solid affects the formation of craters. The existence of a certain amount of nitrogen concentrations in the solid can reduce the crater formation.
4. Vacuum melting process, which has been effective to remove impurities in the materials, may reduce the formation of craters.
5. PBEB irradiation process improves corrosion resistance of machined surfaces of SKD11.
6. From the case study, PBEB irradiation would be a new potential way to finish hard die

and tool steels with high efficiency.

**References:**


[1] N. Taniguchi, Introduction, in: N. Taniguchi, M. Ikeda, I. Miyamoto, T. Miyazaki (eds.), Energy-beam processing of materials: Advanced manufacturing using various energy sources, Oxford University Press, New York, 1989, pp.1-61

[2] S. Schiller, U. Heisig, S. Panzer, Electron beam technology, Wiley, New York, 1982, pp.29-47

[3] S. Schiller, S. Panzer, Thermal surface modification by electron beam high-speed scanning, Annual Review of Materials Science, 18 (1988) 121-140.

[4] D. Dimitrov, M. Aprakova, S. Valkanov, P. Petrov, Electron beam hardening of ion nitrided layers, Vacuum, 49 (1998) 239-246.

[5] R. Günzel, A.I. Rogozin, V.T. Astrelin, Fast, uniform, and large-scale heat treatment by plasma-based electrons, Vacuum, 65 (2002) 59-65.

[6] A. Okada, Y. Uno, K. Nishina, K. Uemura, P. Raharjo, S. Sano, Z. Yu, High efficiency surface finishing of metal mold by large-area electron beam irradiation (2nd Report), Journal of the Japan Society for Precision Engineering, 71 (2005) 1399-1403.

[7] D.I. Proskurovsky, V.P. Rotshtein and G.E. Ozur, Use of low-energy, high-current electron beams for surface treatment of materials, Surface and coatings technology, 96 (1997) 117-122.

[8] Daido Steel Co. Ltd. Home page, 2005, Daido Steel Co. Ltd. Japan, Feb. 2006, <http://www.daido.co.jp/english/products/tool/coldwork_properties.html>

[9] Hitachi metals Co. Japan, Jan. 2001, Some examples of relations between type of resin and selection of steels, Feb. 2006, <http://www.hitachi-metals.co.jp/product/steel/playouto.html>.

[10] H. Fiedler, D. Rumberg, C. Weiss, Electron beam production of steels, in: R.M. Silva (ed), Proceedings of 3rd Electron Beam Processing Seminar, Stratford-upon-Avon, England, 1974, pp. 1c1-1c52.

[11] D. Canadinc, I. Karaman, H. Sehitoglu, Y.I. Chumlyakov, H.J. Maier, The role of nitrogen on the deformation response of hadfield steel single crystals, Metallurgical and Materials Transactions A, 34 (2003) 1821-1831.

[12] Y. Uno, A. Okada, K. Uemura, P. Raharjo, T. Furukawa, K. Karato, High-efficiency finishing process for metal mold by large-area electron beam irradiation, Precision Engineering 29 (2005) 449-455.